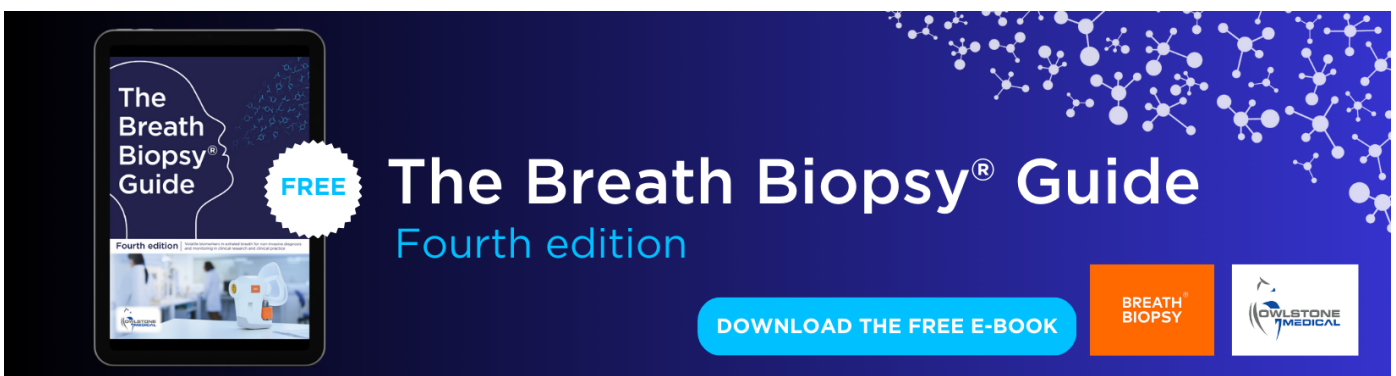**PAPER • OPEN ACCESS**

Combining electrodermal activity analysis and dynamic causal modeling to investigate the visual-odor multimodal integration during face perception

To cite this article: Gianluca Rho *et al* 2024 *J. Neural Eng.* **21** 016020

View the article online for updates and enhancements.

Journal of Neural Engineering

Combining electrodermal activity analysis and dynamic causal modeling to investigate the visual-odor multimodal integration during face perception

Gianluca Rho[1,2,*] ![ORCID], Alejandro Luis Callara[1,2] ![ORCID], Francesco Bossi[1], Dimitri Ognibene[3,4], Cinzia Cecchetto[5], Tommaso Lomonaco[6] ![ORCID], Enzo Pasquale Scilingo[1,2,7] and Alberto Greco[1,2,7]

1 Dipartimento di Ingegneria dell'Informazione, University of Pisa, Pisa, Italy
2 Research Center 'E. Piaggio', School of Engineering, University of Pisa, Pisa, Italy
3 Università Milano-Bicocca, Milan, Italy
4 University of Essex, Colchester, United Kingdom
5 Department of General Psychology, University of Padua, Padua, Italy
6 Department of Chemistry and Industrial Chemistry, University of Pisa, Pisa, Italy
7 These authors contributed equally to this work
* Author to whom any correspondence should be addressed.

E-mail: gianluca.rho@phd.unipi.it

Abstract

Objective. This study presents a novel methodological approach for incorporating information related to the peripheral sympathetic response into the investigation of neural dynamics. Particularly, we explore how hedonic contextual olfactory stimuli influence the processing of neutral faces in terms of sympathetic response, event-related potentials and effective connectivity analysis. The objective is to investigate how the emotional valence of odors influences the cortical connectivity underlying face processing and the role of face-induced sympathetic arousal in this visual-olfactory multimodal integration. *Approach.* To this aim, we combine electrodermal activity (EDA) analysis and dynamic causal modeling to examine changes in cortico-cortical interactions. *Results.* The results reveal that stimuli arising sympathetic EDA responses are associated with a more negative N170 amplitude, which may be a marker of heightened arousal in response to faces. Hedonic odors, on the other hand, lead to a more negative N1 component and a reduced the vertex positive potential when they are unpleasant or pleasant. Concerning connectivity, unpleasant odors strengthen the forward connection from the inferior temporal gyrus (ITG) to the middle temporal gyrus, which is involved in processing changeable facial features. Conversely, the occurrence of sympathetic responses after a stimulus is correlated with an inhibition of this same connection and an enhancement of the backward connection from ITG to the fusiform face gyrus. *Significance.* These findings suggest that unpleasant odors may enhance the interpretation of emotional expressions and mental states, while faces capable of eliciting sympathetic arousal prioritize identity processing.

1. Introduction

The processing of facial expressions is a fundamental mechanism for perceiving others' intentions and emotions [1]. In real-life situations, this process is not limited to the visual system alone but is influenced by contextual information from other sensory channels [2]. Olfactory stimuli have been found to play a crucial role in modulating the hedonic perception of faces [1, 3]. Previous studies have shown that the emotional valence conveyed by contextual odors can affect the recognition of facial expressions and subjective ratings of faces [4–9].

These behavioral responses are accompanied by physiological changes, as evidenced by electroencephalographic (EEG) event-related potential (ERP) studies. These studies have reported an effect of the valence of the odors at both early sensory stages

(P1/N1, N170, and vertex positivity potential (VPP)) [8, 10–12] and later cognitive stages (late positive potential) of face processing [13–15]. However, ERP waveforms reflect the overall activation of the face-perception system, an ensemble of interconnected regions which categorize visual stimuli as faces by analyzing various factors such as expression, gender, and identity [16]. The close association between olfactory and visual areas has been established in previous research [17, 18]. Therefore, investigating the effect of emotional odors on the interactions among the areas of the face-perception system could provide valuable insights into the integration mechanism between olfaction and vision. Such investigations can enhance our understanding of how sensory cues interact to shape our perception of others' facial expressions and emotional states.

The standard ERP analysis based on components' amplitude and latency can not provide a sufficient level of detail to investigate brain dynamics at the network level. Nevertheless, ERPs can be combined with more sophisticated techniques to provide a window on the cortical sources' dynamics underlying face processing. In this context, EEG connectivity analysis allows to investigate the interaction among neuronal assemblies [19]. Particularly, effective connectivity estimates the direct and directional (i.e. causal) influence that a source exerts over another [19]. Among the various effective connectivity approaches [19, 20], dynamic causal modeling (DCM) is a powerful model-based technique designed to test for the effects of experimental factors on the interactions among regions of a specified brain network, starting from observed electrophysiological or functional imaging responses [21, 22]. Several studies applied DCM to reveal the dynamics among sources of the face-perception network either through fMRI [23–27], MEG [28, 29], or intracranial EEG [30] recordings. In this light, DCM can be combined with the information provided by visual ERPs to investigate the modulatory effect of hedonic contextual odors on the cortico-cortical interactions among face-processing areas.

A potential factor of interest in the analysis of the face-odor multimodal integration concerns the arousal elicited by faces. Specifically, within an event-related paradigm, several repetitions of the stimulus are presented over time, and it could be hypothesized that not all the faces are able to elicit the same affective response due to the subjective saliency of facial features [31–33]. This may affect the signal-to-noise ratio (SNR) of the observed ERPs, and potentially reduce or even obscure the modulatory effect of contextual odors on the connectivity. However, although arousal has already been shown to influence face-evoked ERPs [34, 35], its effects when faces are presented with concomitant olfactory stimuli are still poorly investigated. Arousal has a crucial effect on

the processing of external inputs. Motivationally relevant stimuli, such as the perception of a face with specific intrinsic features, are able to generate a transitory and automatic enhancement of arousal [36, 37], that entails a prioritized processing of the stimulus in the visual stream [35]. This mechanism is associated with a series of physiological changes, including a top-down (i.e. endogenous) affective influence on sensory gain control [35], an increase in the amplitude of frequency-specific brain oscillations [32, 38] and in the magnitude of ERP components [34, 35]. In this light, testing for the actual occurrence of enhanced arousal is crucial to ensure that a face has been successfully perceived, thus maximizing the SNR of ERP responses and the consequent effect size of odors' modulation.

Modeling the effects of arousal at both the ERP and DCM connectivity levels requires knowing in advance whether a stimulus has the property of eliciting it. However, such a prior knowledge is far from being easily identified, since particular features that could characterize a perceived stimulus as relevant (e.g. facial identity, eye gaze, expression) may vary on a subjective basis. Besides brain activity, arousal is known to influence autonomic nervous system (ANS) dynamics. Particularly, states of high arousal are associated with an increase of peripheral sympathetic activity [39]. In this light, electrodermal activity (EDA) can be exploited as an objective means to identify the occurrence of enhanced arousal to a given stimulus, possibly related to intrinsic facial features or to emotional expressions [40–43]. EDA is comprised of a slow-varying tonic component overimposed to a fast-varying phasic component. Particularly, the latter is represented by a series of stimulus-evoked skin conductance responses (SCRs), whose elicitation is driven by peripheral sympathetic neural bursts: i.e. the sudomotor nerve activity (SMNA) [39]. Accordingly, sympathetic responses to faces observed from SMNA can be adopted as a reliable marker of enhanced arousal.

In this work, we investigate the effects of hedonic olfactory stimuli and arousal enhancement on face perception, as measured by ERP components and source effective connectivity. Specifically, we hypothesize that odors' valence modulates the strength of specific pathways within the face-perception network, and that arousal evoked by the saliency of faces could play a role on such a multimodal sensory integration. To this aim, we acquired the EDA and EEG signals from 22 healthy volunteers performing a passive visual stimulation task with neutral faces and background pleasant, neutral and unpleasant odors. We propose a novel methodological approach based on the convex-optimization-based EDA (cvxEDA) framework [44] to identify face-evoked peripheral sympathetic responses and characterize the stimuli according to their property of eliciting arousal. The

outcome of this classification procedure is then adopted to model the effects of odors' valence and arousal as between-trial factors on the visual ERP components evoked by faces. We then exploit such ERPs to carry out a DCM and parametric empirical bayes (PEB) analysis of odors and arousal on the connectivity among cortical sources found to be activated by the task. Particularly, PEB allows to build a hierarchical analysis of effective connectivity, where single-subject estimates about neuronal parameters of interest (e.g. connections' strength) are treated as stochastic effects at the group level [45]. To validate our aforementioned hypothesis on the role of enhanced arousal to faces, we aim to assess: (i) whether such mechanism is effectively reflected by the observed ERPs, and (ii) the modulation operated by odors on cortico-cortical interactions at different levels of arousal.

2. Material and methods

2.1. Participants
Twenty-two healthy volunteers (age 27 ± 3, 5 females) were enrolled in the study. Volunteers did not report any history of neurological and cardiovascular diseases, anosmia or being tested positive to COVID-19 over the past 6 months. Volunteers were not allowed to have any food nor drink in the 30 min preceding the experiment. The study was conducted according with the guidelines of the Declaration of Helsinki and approved by the Bioethics Committee of the University of Pisa Review No. 14/2019, 3 May 2019. All participants gave written informed consent to participate in the study.

2.2. Olfactory stimuli
We selected three different odorants: i.e. banana (isoamyl acetate; $CH_3COOCH_2CH_2CH(CH_3)_2$), isovaleric acid (($CH_3)_2CHCH_2COOH$), and n-butanol ($CH_3CH_2CH_2CH_2OH$). We chose such odorants to convey positive (banana), negative (isovaleric acid), and neutral (n-butanol) valence according to previous literature results [46, 47]. For each subject, we prepared 1 ml isointense solutions diluting pure odorant substances in distilled water according to the ratios of 1/20 (banana, n-butanol) and 1/10 (isovaleric acid) respectively. Odorants were delivered through an in-house built computer-controlled olfactometer at a flow rate of 60 ml min^{-1}.

2.3. Olfactometer device
The 4-channels computer-controlled olfactometer used herein is composed by (i) a pressure regulator to set air pressure at 7 Bar, (ii) four stainless-steel containers (50 ml) equipped with o-rings, stainless steel caps and clamping rings to ensure a gas-tight closure, (iii) 10 low dead-volume three-way solenoid valves (Parker Hannifin, Italy), (iv) a digital flow meter (Honeywell, Italy), and (v) a disposable nasal
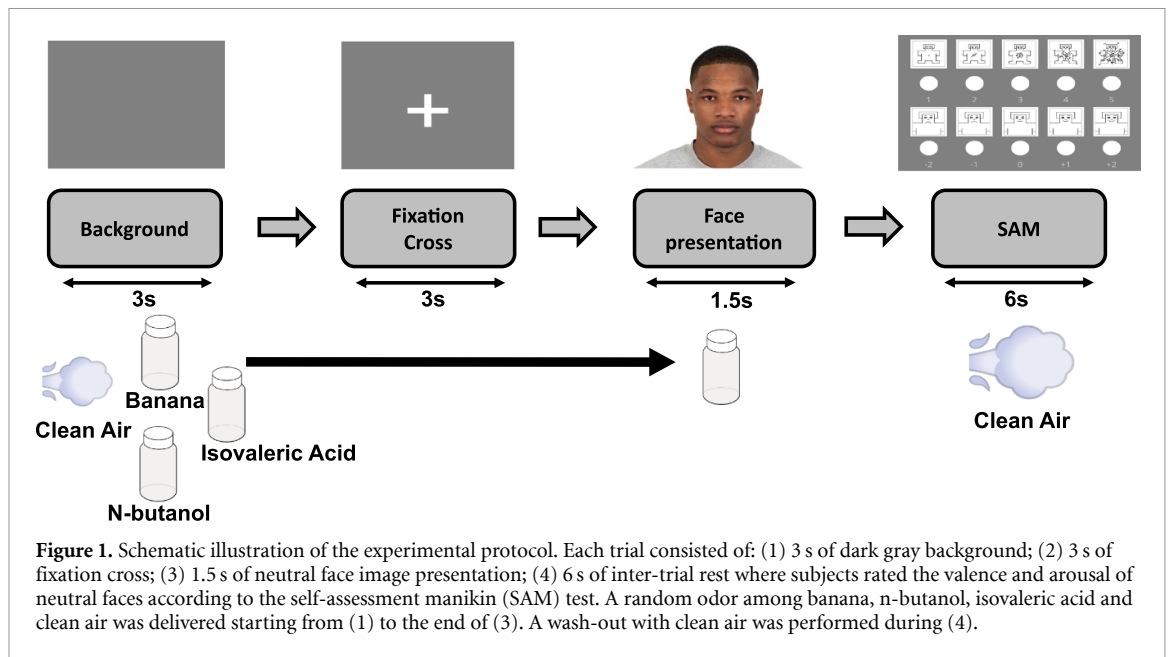
cannula. An Arduino in-house code controlled the solenoid valves allowing them being opened and closed through a well-defined sequence of actions. The software allows the delivery of pure clean air (i.e. all valves are opened) or odors kept at room temperature within the containers. Components were connected to each other using polytetrafluoroethylene (PTFE) fittings and tubings (internal diameter of 0.3 mm) to reduce the olfactometer dead-volume up to 1 ml. The nasal cannula is connected to the olfactometer though a 3 m long PTFE line. The olfactometer showed a negligible memory effect and a low background emissions of chemicals in the air/odors mainstream as determined by thermal desorption coupled to gas-chromatography and mass spectrometry protocol [48], an overall air flow delivery variability less than 1%, and a rise time (10%–90% of the final value) close to 300 ms.

2.4. Visual stimuli
For the visual stimuli of neutral faces, we used the Chicago Face Database [49]. We chose 128 different actors showing a neutral expressions. Particularly, we selected a balanced number of actors across gender, age, and ethnicity, to mitigate potential confounding effects related to the intrinsic characteristics of the actors. The pictures were presented in a completely randomized order with respect to the olfactory condition. The visual stimuli were shown on a 15″ laptop screen with a refresh rate of 60 Hz and a resolution of 1920×1080. The pictures' size was 15 cm in width and 10 cm in height, and were displayed at about 50 cm from the eyes of the participants, resulting in a visual angle of about 17°.

2.5. Experimental protocol
The experimental protocol was divided into two parts. In the first part of the experiment, we collected the subjective ratings of the odorants. To this aim, we presented the olfactory stimuli (i.e. n-butanol, banana and isovaleric acid) to the volunteers in a randomized order for a duration of 10 s, and we asked them to evaluate them in terms of valence (from -2 to $+2$) and arousal (from 1 to 5) according to the self-sssessment Manikin (SAM) test [50]. Two participants were not able to perceive any of the administered odorants and have been excluded from the experiment, resulting in a final panel of 20 volunteers (age 26 ± 3, 5 females). In the second part of the experiment, we designed an experimental protocol comprised of 128 trials. As schematically reported in figure 1, each trial consisted of: (1) 3 s of dark gray background; (2) 3 s of a dark gray background with a white fixation cross; (3) 1.5 s of neutral face image presentation; (4) 6 s of inter-trial rest. Within each inter-trial rest, subjects were asked to evaluate the facial expression in terms of valence and arousal according to the SAM test, through an interactive

Figure 1. Schematic illustration of the experimental protocol. Each trial consisted of: (1) 3 s of dark gray background; (2) 3 s of fixation cross; (3) 1.5 s of neutral face image presentation; (4) 6 s of inter-trial rest where subjects rated the valence and arousal of neutral faces according to the self-assessment manikin (SAM) test. A random odor among banana, n-butanol, isovaleric acid and clean air was delivered starting from (1) to the end of (3). A wash-out with clean air was performed during (4).

interface. The facial images were presented in combination with clean air or one of the three different odorants rated in the first part of the experiment, for a total of $128/4 = 32$ trials for each olfactory condition. Each odorant was delivered starting from the onset of the dark gray background to the end of the visual stimulus. A wash-out with clean air was performed during the inter-trial rest. We presented both visual and olfactory stimuli in a randomized order through the PsychoPy software [50]. A custom-made analogic front-end circuit controlled the precise timing for the administration of both the visual and olfactory stimuli.

2.6. EEG and EDA acquisition
EEG signal was acquired using a high-density 128-channel geodesic EEG System 300 from Electrical Geodesic, Inc. (EGI). Electrodes were grounded through two additional channels placed between Cz and Pz and referenced through Cz. We always kept electrode impedances below $20 \, \text{k}\Omega$ during the acquisitions. EEG was acquired at the sampling frequency of 500 Hz.
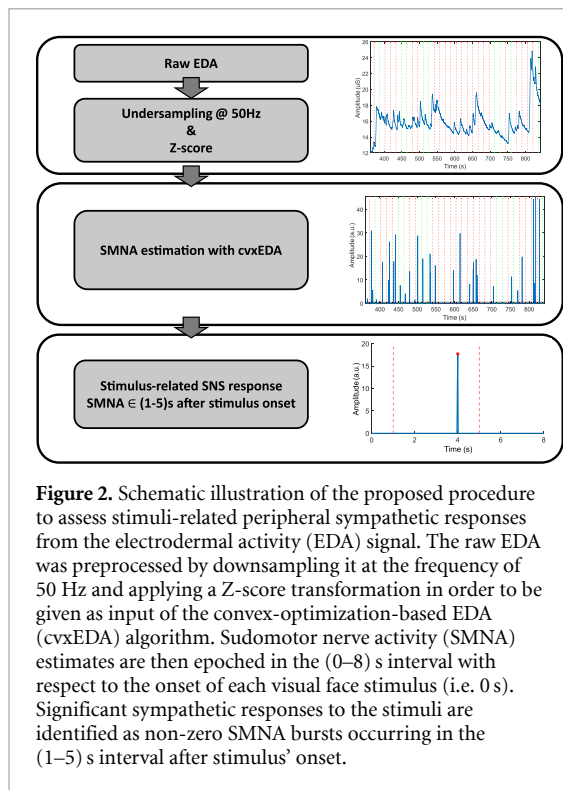
EDA was acquired using a Shimmer3 GSR+ unit (Shimmer, USA) at the sampling frequency of 250 Hz. We recorded EDA through a pair of Ag/AgCl electrodes placed on the proximal phalanx of the first and second fingers of the non-dominant hand, respectively.

2.7. EDA-driven sympathetic activity estimation
We implemented a procedure based on the analysis of EDA signal to estimate the occurrence of enhanced sympathetic responses associated with the visual presentation of faces. A well-known problem in EDA analysis concerns the temporal overlapping

of consecutive SCRs, which may hamper the association between a given response and its potential triggering stimulus [39, 44, 51]. To address this issue, we adopted the cvxEDA [44] model to recover an estimate of the SMNA from the observed EDA responses. Specifically, cvxEDA considers that each SCR is preceded in time by sparse and discrete bursts of SMNA. These bursts are characterized by a higher temporal resolution compared to phasic activity, and can thus be exploited to identify the time instants at which peripheral sympathetic responses evoked by faces occur [44]. Accordingly, we assumed that visual stimuli eliciting an enhanced peripheral sympathetic response could be followed by the occurrence of an SCR and, thus, a non-zero SMNA neural burst.

Operationally, for each subject and for each odor condition (i.e. pleasant, unpleasant, neutral, air), we undersampled the EDA to the sampling frequency of 50 Hz, and we performed a Z-scoring on the data [44]. Then, we applied cvxEDA to obtain an estimate of the SMNA. We set the sparsity parameter of the model to 8×10^{-3}, as a trade-off between noise-suppression and distortion of the solution. Indeed, larger values of this parameter yield to a higher sparsity of SMNA responses and thus to a stronger suppression of noise-induced spikes, but also more attenuation of true physiological responses. On the other hand, smaller values yield to a less distorted but noisier solution [44]. We set the other model's parameters at their default value. We identified discrete events of enhanced sympathetic arousal associated with the presentation of visual stimuli as those epochs having non-zero SMNA bursts occurring in the (1–5) s after stimulus onset. This choice is supported by several studies indicating that a stimulus-evoked SCR

Figure 2. Schematic illustration of the proposed procedure to assess stimuli-related peripheral sympathetic responses from the electrodermal activity (EDA) signal. The raw EDA was preprocessed by downsampling it at the frequency of 50 Hz and applying a Z-score transformation in order to be given as input of the convex-optimization-based EDA (cvxEDA) algorithm. Sudomotor nerve activity (SMNA) estimates are then epoched in the (0–8) s interval with respect to the onset of each visual face stimulus (i.e. 0 s). Significant sympathetic responses to the stimuli are identified as non-zero SMNA bursts occurring in the (1–5) s interval after stimulus' onset.

is observed to occur within that range of latency after stimulus' onset [39, 52]. A schematic illustration of the procedure is reported in figure 2.

For each odor condition, we then extracted: (1) the number of epochs with/without a stimulus-related sympathetic response (nSymp), (2) the average latency of sympathetic responses, (3) the average amplitude of the SMNA, computed as the average amplitude across epochs and then over time, and (4) the subject-average SCR generated by the SMNA bursts.

2.8. EEG preprocessing

We preprocessed the EEG signal using EEGLAB [53]. First, we filtered the data with a zero-phase low-pass antialiasing filter and then undersampled it to the sampling frequency of 100 Hz. Afterwards, we applied a zero-phase high-pass filter at the cutoff frequency of 0.1 Hz to improve data stationarity. We removed flat and poorly correlated channels by exploiting the method presented in [54]. Specifically, each channel was compared with its reconstructed version obtained from the spherical interpolation of its neighbors and was removed if the correlation coefficient was less than a user-defined threshold. Here, we used a correlation threshold of 0.8. After visual inspection, we recovered the removed channels through spherical interpolation, and we re-referenced the data to its average. We decomposed EEG data through independent component analysis (ICA) [55], and we removed independent components (ICs) resembling artifact activity (e.g. muscular, eye-blinks and other

sources of noise) through visual inspection of their associated time course, scalp map, and power spectrum. For each subject, we then epoched the EEG signal in the $(-200, 1000)$ ms range with respect to the onset of visual stimuli (i.e. 0 ms), and we visually inspected the data to remove epochs containing residual artifact activity. An average number of 125 epochs (minimum retained: 99; maximum retained: 128) was retained over the subjects. Finally, clean EEG epochs were corrected for their baseline (i.e. from -200 ms to 0 ms) and low-pass filtered at the cutoff frequency of 30 Hz using default settings in EEGLAB. We grouped the epochs according to the odor condition, and we further distinguished them based on the presence or absence of a peripheral sympathetic activation (hereinafter referred to as *Symp* condition). Accordingly, we obtained subject-average ERPs for a total of 8 conditions: clean air, n-butanol, banana, and isovaleric acid, with/without the presence of a sympathetic response.

We focused on relevant ERP components associated with the visual processing of faces, as well as their typical regions of interest (ROIs) on the scalp, based on the previous literature [8, 10, 11, 15, 16, 56, 57] (see table 1 for details). Specifically, we extracted: (1) the P1 component in the 120–160 ms interval after stimulus onset in the occipital region around O1 and O2, (2) the N1 component at the same latency as P1, in the central region around Cz, (3) the right/left N170 component in the 160–200 ms interval after stimulus onset in the parieto-temporal regions near P7 and P8, respectively, and (4) the Vertex Positive Potential (VPP) in the 160–200 ms interval after stimulus onset in the same ROI of the N1 component. Moreover, for a comparison with the previous literature, we also identified: (5) the P2 component at 220–300 ms after stimulus onset in the same ROI of P1, and (6) the late positive potential (LPP), a sustained positivity at 300–500 ms after stimulus onset around Pz. For each subject and for each of these components, we extracted the mean amplitudes across the respective time intervals and ROIs.

2.9. Statistical analysis on self-report, EDA and ERP data

We investigated for possible differences in the valence and arousal subjective ratings of olfactory stimuli through multiple Wilcoxon sign-rank tests, with a significance level of $\alpha = 0.05$. *P*-values were adjusted for multiple comparisons testing with Bonferroni correction. We further tested for the influence of the odors and sympathetic responses on the valence and arousal ratings of faces using linear mixed effect models (LMMs). Given the lack of consensus regarding the most appropriate use of LMMs in the literature (see e.g. [58, 59]), we built our models according to the following rationale: first, we included all of the fixed effects that allowed the model to converge,

Table 1. Channels region of interest (ROI) and time interval (ms) for each of the investigated event-related potential (ERP) components (i.e. P1, N1, right N170 (rN170), left N170 (lN170), vertex positive potential (VPP), P2, and late positive potential (LPP)). The amplitude of each ERP component was obtained as the average over the corresponding ROI and time interval reported in the table. Channels' name is reported according to the geodesic EGI 128-channels cap.

	Channels	Time interval
P1	E59 E65 E66 E70 E71 E76 E83 E84 E90 E91	120–160 ms
N1	E6 E7 E13 E30 E31 E37 E54 E55 E79 E80 E87 E105 E106 E112 E129	120–160 ms
rN170	E96 E97 E101 E102 E108	160–200 ms
lN170	E45 E46 E50 E51 E58	160–200 ms
VPP	E7 E13 E30 E31 E37 E54 E55 E79 E80 E87 E105 E106 E112 E129	160–200 ms
P2	E59 E65 E66 E70 E71 E76 E83 E84 E90 E91	220–300 ms
LPP	E52 E53 E60 E61 E62 E67 E77 E78 E85 E86 E92	300–500 ms

leading to a full-factorial model. Concerning random effects, we only included those that presented a correlation $|\rho| < 0.80$ with other random effects. This, one the one hand, avoided problems associated with model converge and overfitting. On the other hand, it allowed to obtain reliable estimates from the analysis of fixed effects [60]. The significance of each effect was estimated using the Satterthwaite approximation for degrees of freedom. Accordingly, we built two distinct random-intercept LMMs, modeling the valence and arousal ratings of faces, respectively, with Odor (i.e. clean air, butanol, banana, isovaleric acid), Symp (i.e. presence/absence of a sympathetic response) and their two-way interaction as fixed effects ($\alpha < 0.05.$):

$$\text{SAM}_i = \text{Odor} * \text{Symp} + (1|\text{SubjectID}) \qquad (1)$$

where SAM_i is either the valence or arousal subjective rating of faces, $\text{Odor} * \text{Symp}$ is the two-way interaction between fixed effects, and $(1|\text{SubjectID})$ is the random intercept for each subject. We could not include any of Odor and Symp among random effects, as they resulted in over-threshold (i.e. $|\rho| > 0.80$) multiple collinearities that hampered model convergence.

Concerning the physiological data, we tested for a significant effect of the odors on the SMNA. To this aim, we conducted a 1×4 within-subject repeated-measure ANOVA on both the amplitude and the latency of SMNA responses, with Odor as the main effect ($\alpha = 0.05$). Multiple comparison testing was controlled with false-discovery rate (FDR) for multiple testing under dependency [61]. We further tested for an interaction between the occurrence of sympathetic responses and the olfactory stimuli through a within-subject two-way ANOVA on the number of EDA epochs grouped by odor condition (i.e. clean-air, n-butanol, banana, isovaleric acid) and the presence/absence of an SMNA response, respectively ($\alpha = 0.05$).

Finally, we tested for a significant effect of contextual odors and sympathetic responses on the amplitude of the ERP components described in section 2.8. To this aim, we followed the methodology explained previously to model the amplitude

of each ERP component through a random-intercept LMM, with Odor (i.e. clean air, butanol, banana, isovaleric acid), Symp (i.e. presence/absence of a sympathetic response) and their two-way interaction as fixed effects:

$$\text{ERP}_i = \text{Odor} * \text{Symp} + (1|\text{SubjectID}) . \qquad (2)$$

Where ERP_i is the amplitude of the ith ERP component, $\text{Odor} * \text{Symp}$ represents the two-way interaction between fixed effects, and $(1|\text{SubjectID})$ represents the random intercept for each subject. We could not include either the effect of Odor or the effect of Symp among random effects, as they showed over-threshold (i.e. $|\rho| > 0.80$) multiple collinearities. Indeed, on the one hand, that would not have allowed the model to converge. On the other hand, collinearities would have compromised the results of fixed-effects analysis. Post-hoc comparisons were conducted with pairwise t-tests, and the resulting p-values were adjusted with the Bonferroni correction ($\alpha = 0.05$).

2.10. Effective connectivity analysis with DCM

The analysis of effective connectivity was carried out using SPM12 [62].

We used DCM for ERPs [22, 63] to investigate the modulatory effect of odors and sympathetic responses on the effective connectivity. Specifically, DCM models the observed ERPs by combining a physiologically plausible neuronal model of interacting cortical regions, and a spatial forward model that maps the cortical activity to observed EEG data. Each region is described by three interconnected neuronal subpopulations: interneurons, spiny stellate cells, and pyramidal neurons. Regions are coupled to each other through extrinsic connections, that are distinguished into forward, backward, and lateral according to the hierarchical organization of the cortex [64]. The effect of administered sensory stimuli on neuronal dynamics is accounted for through specific input connections modeling the afferent activity relayed by subcortical structures to the spiny stellate layer of target cortical regions [22, 63]. Notably, such inputs are the same for each experimental condition. Accordingly, differences among ERPs due to either contextual

or stimulus attributes are explained by modulatory coupling gains on the connection strengths [22, 63]. The activity of pyramidal neurons from each region is then projected to the EEG channels through an electromagnetic forward model which accounts for the field spread effects in the head.

2.10.1. Network specification

The DCM for ERP framework explains ERP dynamics as arising from a small number of brain regions [65]. The selection of which brain regions to include in the network for DCM analysis can be made using either prior knowledge from the literature or source reconstruction techniques. Here, we adopted a group source reconstruction approach based on multiple sparse priors (MSP) implemented in SPM12 [66]. Particularly, while MSP has been shown to potentially reduce localization error with high-density EEG systems [66], group-inversion yields better results compared to individual inversions by introducing additional constraints on the set of sources explaining subjects' data [67]. Operationally, we used channels' position co-registered to the MNI standard head template as provided by SPM. Then, we inverted ERPs activity on a cortical mesh comprising 8196 dipoles in the time range from -200 to 400 ms. For each subject, we then created contrasts of log power differences in the 0–400 ms time range, collapsed over the experimental conditions, against the prestimulus window (i.e. -200 to 0 ms). These contrast images were smoothed with an 8 mm Gaussian kernel to create a 3D volumetric NIFTI image. Images were entered into a one-sample t-test design in SPM12 and we tested for significant changes in power with respect to the prestimulus through an F-contrast. Significant regions ($p < 0.05$; family-wise error rate corrected at the cluster level) were labeled according with the automated anatomical labeling (AAL) atlas [68].

2.10.2. DCM subject-level connectivity analysis

We performed DCM analysis on the subject-average ERPs relative to the odor conditions, and with and without a sympathetic response. Accordingly, for each subject, we specified a factor analysis on the single-subject connectivity, with Odor and Symp as between-trial factors. We reduced the data to the first four principal components (PC) or modes of EEG channels' mixture. Such a choice is a trade-off between the computational cost of DCM model inversion and the percentage of variance explained by the data [69–71]. Notably, reducing ERP data to their first four PC is indicated as sufficient to capture the components of interest [63]. We focused model inversion on the 0–400 ms time window with respect to the stimulus onset, through a Hanning window. Finally, we adopted the ERP neural mass model (NMM) to model temporal dynamics within and between the network sources.

Concerning the forward model, we modeled the spatial activity of brain sources as equivalent current dipoles (ECD option in SPM12) on the cortex. The passive volume conduction effects on the dipoles' electric field were modeled through a BEM model of the head made of three layers, i.e. cortex, skull and brain, whose conductances were set to 0.33, 0.0042 and 0.33 S m^{-1}, respectively.

We allowed the effect of both Odor and Symp to modulate all the connections of the network, including self-inhibitory effects on each node.

2.10.3. PEB group-level connectivity analysis

We inferred the significant modulatory effects of Odor and Symp on the group-level connectivity through the PEB framework [45, 72]. Such a framework allows to build statistical hierarchical models where single-subject DCM parameters of interest can be treated as random effects on the group-level connectivity:

$$Y_i = \Gamma\left(\theta_i^{(1)}\right) + \epsilon_i^{(1)} \tag{3}$$

$$\theta^{(1)} = (X_b \otimes X_w)\,\theta^{(2)} + \epsilon^{(2)}. \tag{4}$$

More specifically, single-subject ERPs Y_i are explained by a DCM $\Gamma(.)$ with unknown parameters $\theta_i^{(1)}$, plus a zero-mean white Gaussian noise residual $\epsilon^{(1)}$. Parameter estimates of interest are then grouped together across subjects (i.e. $\theta_i^{(1)}$) and modeled at the group-level (4) through a general linear model having design matrix $X = (X_b \otimes X_w)$ and group parameters $\theta^{(2)}$. The X_b matrix models the between-subject effects, whereas the X_w matrix models which single-subject parameters are influenced by such effects. The $\otimes$ symbol denotes the Kronecker product. Any unexplained between-subject difference (e.g. non-modeled sources of variations, random effects) is modeled by the zero-mean white Gaussian residuals $\epsilon^{(2)}$.

We grouped together the single-subject estimates associated with the modulatory effect of *Odor* and Symp such that $\theta^{(1)} = [\theta_{\text{Odor}}^{(1)}, \theta_{\text{Symp}}^{(1)}]^T$, and we fitted a PEB model with between-subject design matrix $X_b = 1^T$ and within-subject design matrix $X_w = I$ to estimate the average effect of such conditions on each connection of the group connectivity.

We then applied a greedy search to infer the best combination of group-level parameters $\theta^{(2)}$ describing the average effects of Odor and Symp. Specifically, we iteratively applied Bayesian model reduction (BMR) to obtain an estimate of nested PEB models with/without a particular set of connections, as well as their posterior probability (Pp) of being the best model describing the observed data [73]. We then computed a Bayesian model average (BMA) over the models resulted from the last iteration of

greedy-search procedure. BMA performs an average of the parameter posterior densities across models, weighted for their *Pp*. Accordingly, we obtained a set of group-level parameters whose value is no longer conditional on the particular model assumed. Finally, we thresholded the BMA results pruning away those parameters having a *Pp* of being modulated by either *Odor* or *Symp* lower than 0.95. We based such thresholding on the free-energy of the models estimated during the BMR procedure (see appendix 3 of [45]).

2.11. DCM connectivity analysis summary
In this section, we resume the main steps and key parameters of the connectivity analysis with DCM. For each subject, we performed the following operations:

- reduction of subject-average ERP data to the first 4 PCs of EEG channels' mixture;
- selection of the (0–400) ms time interval of ERPs through a Hanning window;
- specification of the model design matrix with Odor and Symp as between-trial factors;
- definition of the network nodes' position in the MNI space, as well as their hierarchical connections. All the connections are allowed to be modulated by Odor and Symp;
- selection of the ERP NMM to model sources' dynamics;
- specification of the standard forward model provided by SPM12 with the ECD option (head model: standard MNI template; three-layer BEM for volume conduction effects, with cortex, skull and brain conductance set to 0.33, 0.0042 and 0.33 S m^{-1}, respectively).

The parameters related to the modulatory effect of the Odor and Symp conditions were collated together across subjects, to infer their average modulatory effect on the group-level connectivity with PEB. To this aim, we performed the following steps:

- definition of $X_b = 1^T$;
- definition of $X_w = I$;
- greedy search with BMR on the PEB model estimates, and BMA across the explored model space;
- rejecting BMA parameters (i.e. connections) having $Pp < 0.95$ of being present vs. absent, based on the free-energy principle.

3. Results

3.1. SAM statistical analysis results
In figure 3 we report the statistical analysis results of the SAM on the administered odorants (mean ± standard error (SE)). Subjects rated isovaleric acid as significantly more unpleasant

(valence $= -0.62 \pm 0.18$; figure 3(a)) and more arousing (arousal $= 2.81 \pm 0.22$; figure 3(b)) compared to banana and n-butanol. We did not find any significant differences between the valence and arousal ratings of banana (valence $= 0.38 \pm 0.20$; arousal $= 2.33 \pm 0.21$) and n-butanol (valence $= 0.10 \pm 0.18$; arousal $= 1.86 \pm 0.17$).

Concerning the subjective ratings of faces, we did not find any significant effect for the Odor condition on both the valence ($F_{3,19} = 1.3412, p > 0.05$) and arousal ($F_{3,19} = 1.3892, p > 0.05$) ratings. Similarly, we did not find any significant effect for the Symp condition on both valence ($F_{3,19} = 0.2323, p > 0.05$) and arousal ($F_{3,19} = 0.0962, p > 0.05$) ratings.
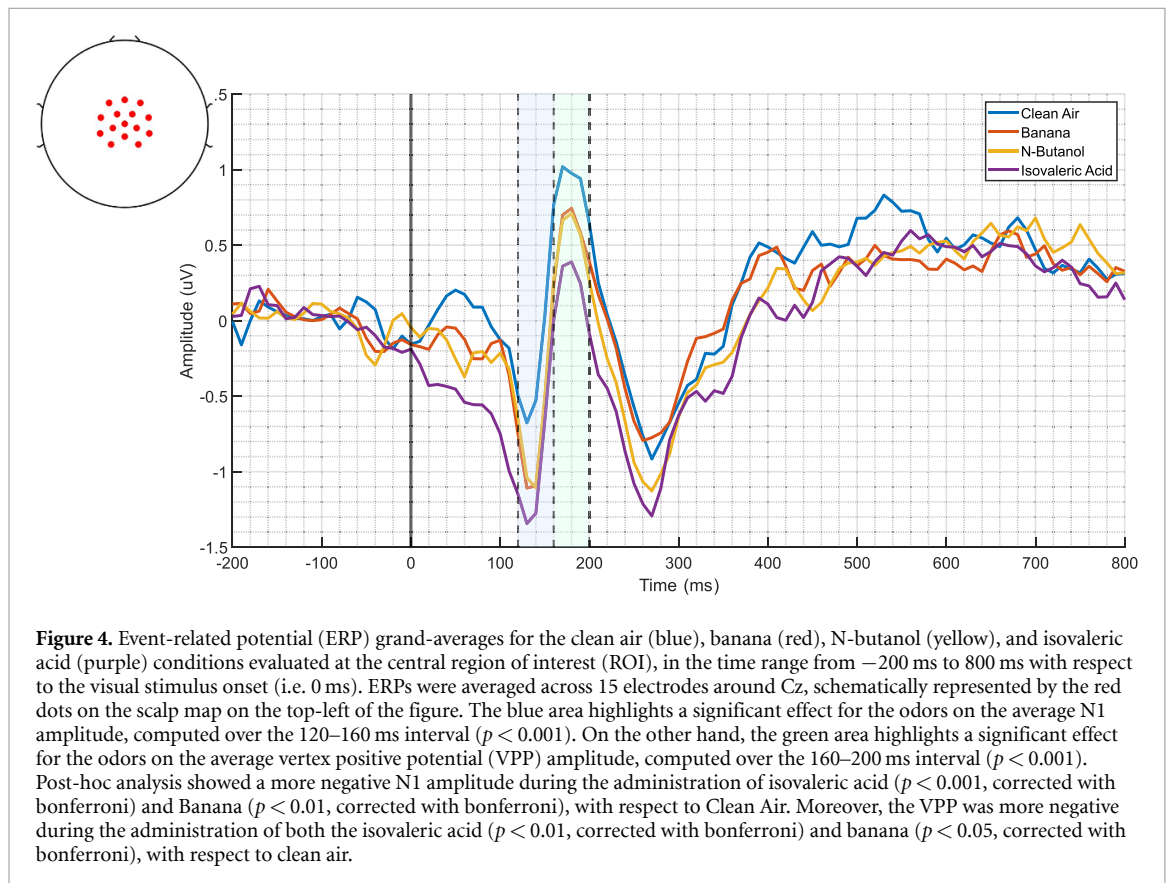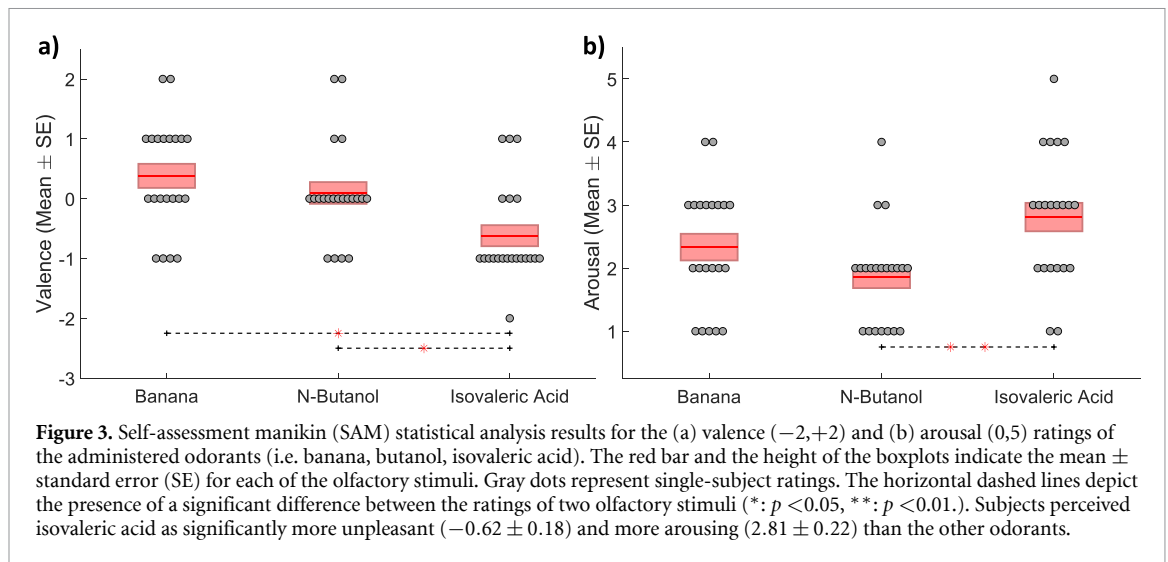
3.2. EDA statistical analysis results
We did not find any significant differences among odor conditions neither for the average amplitude nor the latency of SMNA responses. Conversely, we found a significant effect of nSymp following the 2×4 ANOVA ($F_{6,64} = 5.76, p < 10^{-5}$; FDR-corrected). More specifically, we found a lower number of stimuli associated with a sympathetic response (mean ± standard deviation; 11.76 ± 3.06), compared to the stimuli without the manifestation of a sympathetic response (19.61 ± 2.63), irrespective of the odor condition.

3.3. ERP statistical analysis results
The modeling of ERP components' amplitude with the random-intercept LMMs highlighted a significant effect for the Odor condition on the N1 ($F_{3,133} = 6.1261, p < 0.001$) and the VPP ($F_{3,133} = 4.6851, p < 0.001$) components at the central ROI around the Cz channel. In figure 4, we report the grand-average ERP for each of the odor conditions, together with the N1 and VPP significant intervals highlighted in blue and green, respectively, and a schematic representation of the ROI on the scalp map. Post-hoc analysis highlighted a more negative N1 amplitude during the administration of isovaleric acid ($t_{133} = 3.998; p < 0.001$) and banana ($t_{133} = 3.333; p < 0.01$), with respect to clean air. Moreover, we observed a more negative VPP amplitude during the administration of both isovaleric acid ($t_{133} = 3.535; p < 0.01$) and banana ($t_{133} = 2.846; p < 0.05$), with respect to clean air.

Moreover, we observed a significant effect for the Symp condition on the amplitude of the left N170 component ($F_{1,133} = 10.8749, p < 0.001$). In figure 5 we report the grand-average ERP evaluated at the ROI around P7, for each of the combinations between Odor and Symp conditions. As depicted in the figure, the presence of a sympathetic response resulted in more negative N170 component, with respect to the absence of a sympathetic response, irrespective of the
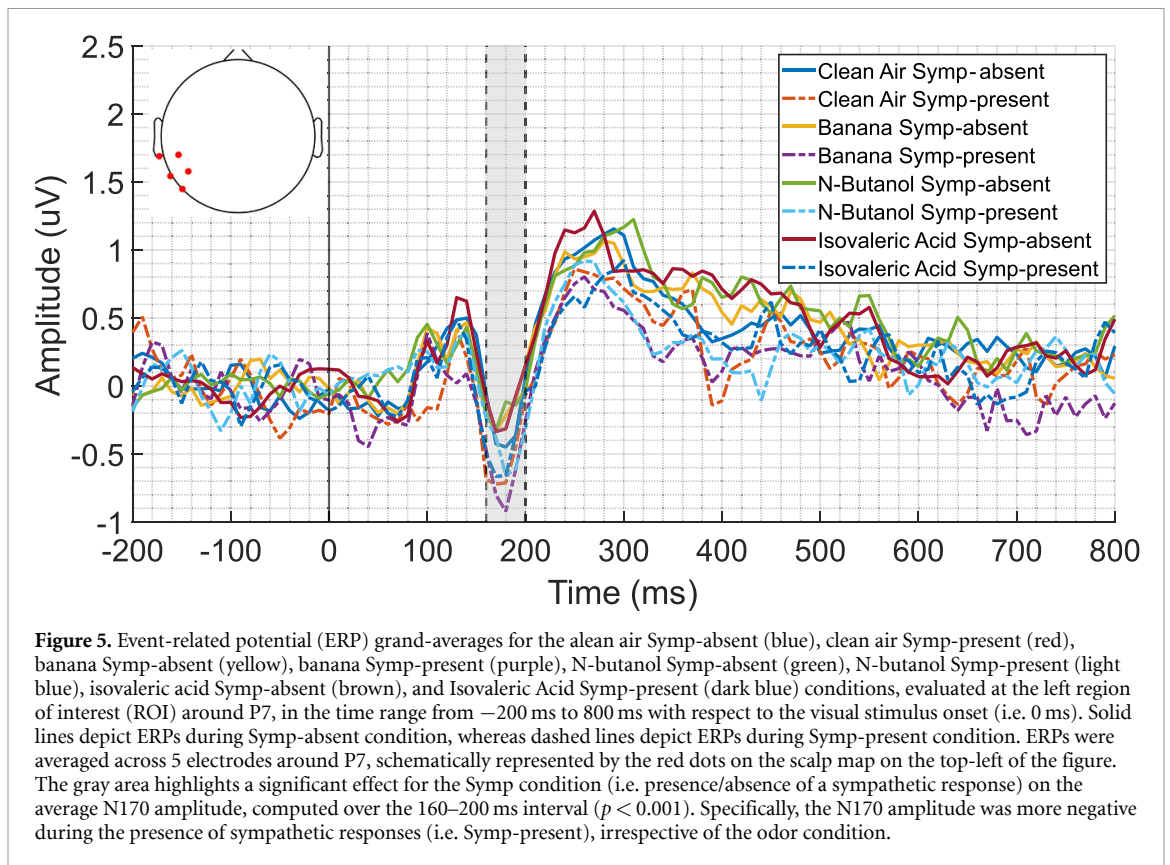
Figure 3. Self-assessment manikin (SAM) statistical analysis results for the (a) valence (-2,$+2$) and (b) arousal (0,5) ratings of the administered odorants (i.e. banana, butanol, isovaleric acid). The red bar and the height of the boxplots indicate the mean $\pm$ standard error (SE) for each of the olfactory stimuli. Gray dots represent single-subject ratings. The horizontal dashed lines depict the presence of a significant difference between the ratings of two olfactory stimuli (*: $p < 0.05$, **: $p < 0.01$.). Subjects perceived isovaleric acid as significantly more unpleasant (-0.62 ± 0.18) and more arousing (2.81 ± 0.22) than the other odorants.

Figure 4. Event-related potential (ERP) grand-averages for the clean air (blue), banana (red), N-butanol (yellow), and isovaleric acid (purple) conditions evaluated at the central region of interest (ROI), in the time range from -200 ms to 800 ms with respect to the visual stimulus onset (i.e. 0 ms). ERPs were averaged across 15 electrodes around Cz, schematically represented by the red dots on the scalp map on the top-left of the figure. The blue area highlights a significant effect for the odors on the average N1 amplitude, computed over the 120–160 ms interval ($p < 0.001$). On the other hand, the green area highlights a significant effect for the odors on the average vertex positive potential (VPP) amplitude, computed over the 160–200 ms interval ($p < 0.001$). Post-hoc analysis showed a more negative N1 amplitude during the administration of isovaleric acid ($p < 0.001$, corrected with bonferroni) and Banana ($p < 0.01$, corrected with bonferroni), with respect to Clean Air. Moreover, the VPP was more negative during the administration of both the isovaleric acid ($p < 0.01$, corrected with bonferroni) and banana ($p < 0.05$, corrected with bonferroni), with respect to clean air.

contextual olfactory stimulus. We did not find a significant interaction between *Odor* and *Symp* for any of the ERP components investigated.

3.4. Network identification results

We found activation of the right inferior occipital gyrus (rIOG; MNI coordinates: 48 -76 -2), right Fusiform Gyrus (rFFG; MNI coordinates: 38 -18 -32), right and left inferior temporal gyrus (rITG; MNI coordinates: 52 -38 -20; lITG; MNI coordinates: -50 -38 -22), right and left middle temporal gyrus (rMTG; MNI coordinates: 52 -62 14; lMTG; MNI coordinates: -54 -64 10), and right secondary visual cortex (rVII; MNI coordinates: -10 -98 -10) ($p < 0.05$; family-wise error rate corrected at the cluster level).

We specified the network for DCM analysis focusing on the IOG, FFG, ITG, and MTG for their central role in the processing of faces and their role in the integration of visual and olfactory stimuli [25, 26, 74–77]. Furthermore, in line with the previous literature, we focused on the
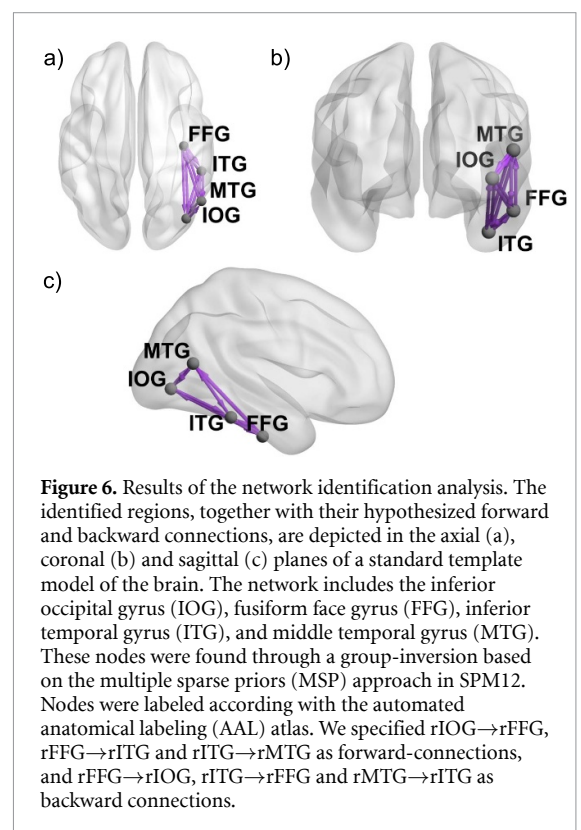
Figure 5. Event-related potential (ERP) grand-averages for the alean air Symp-absent (blue), clean air Symp-present (red), banana Symp-absent (yellow), banana Symp-present (purple), N-butanol Symp-absent (green), N-butanol Symp-present (light blue), isovaleric acid Symp-absent (brown), and Isovaleric Acid Symp-present (dark blue) conditions, evaluated at the left region of interest (ROI) around P7, in the time range from −200 ms to 800 ms with respect to the visual stimulus onset (i.e. 0 ms). Solid lines depict ERPs during Symp-absent condition, whereas dashed lines depict ERPs during Symp-present condition. ERPs were averaged across 5 electrodes around P7, schematically represented by the red dots on the scalp map on the top-left of the figure. The gray area highlights a significant effect for the Symp condition (i.e. presence/absence of a sympathetic response) on the average N170 amplitude, computed over the 160–200 ms interval ($p < 0.001$). Specifically, the N170 amplitude was more negative during the presence of sympathetic responses (i.e. Symp-present), irrespective of the odor condition.

right visual stream of face processing [24, 25, 74, 78, 79]. We specified rIOG→rFFG, rFFG→rITG and rITG→rMTG as forward-connections, and rFFG→rIOG, rITG→rFFG and rMTG→rITG as backward connections according with previously reported evidence on the nodes' hierarchical structure [24, 25, 80–82] (figure 6). We hypothesized IOG as the first stage responsible for face processing in our network [24, 26, 83, 84]. Accordingly, we modeled the effect of the thalamic sensory input relay of 'faces' directly entering the IOG (i.e. the network input).

3.5. DCM subject-level connectivity analysis

Following the results of SAM and ERP analysis, we decided to focus our connectivity study on the effects of isovaleric acid and arousal enhancement on the visual processing of faces. Accordingly, we built a 2 × 2 factorial DCM analysis with factors Odor (i.e. clean air vs. isovaleric acid) and Symp (i.e. sympathetic vs. no sympathetic response). For each subject, the DCM model was successfully fitted to the observed data without observing any problem of early convergence. The models showed a good representation of the data, with an average explained variance of 90.77%.

In figure 7 we report the result of the ERP reduction to the first four principal modes of EEG channels' mixture, together with the modes predicted by the model, for an exemplary subject. As depicted, PCA channels' reduction yielded a parsimonious yet efficient representation of the data. Specifically, the first

Figure 6. Results of the network identification analysis. The identified regions, together with their hypothesized forward and backward connections, are depicted in the axial (a), coronal (b) and sagittal (c) planes of a standard template model of the brain. The network includes the inferior occipital gyrus (IOG), fusiform face gyrus (FFG), inferior temporal gyrus (ITG), and middle temporal gyrus (MTG). These nodes were found through a group-inversion based on the multiple sparse priors (MSP) approach in SPM12. Nodes were labeled according with the automated anatomical labeling (AAL) atlas. We specified rIOG→rFFG, rFFG→rITG and rITG→rMTG as forward-connections, and rFFG→rIOG, rITG→rFFG and rMTG→rITG as backward connections.

three EEG modes represented data variance associated with the P1, N170, and P2 components, whereas the fourth mode represented data variance mainly
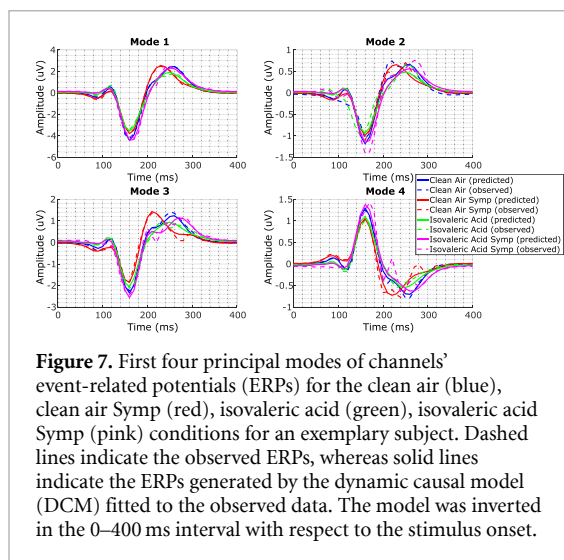
Figure 7. First four principal modes of channels' event-related potentials (ERPs) for the clean air (blue), clean air Symp (red), isovaleric acid (green), isovaleric acid Symp (pink) conditions for an exemplary subject. Dashed lines indicate the observed ERPs, whereas solid lines indicate the ERPs generated by the dynamic causal model (DCM) fitted to the observed data. The model was inverted in the 0–400 ms interval with respect to the stimulus onset.

associated with the VPP. Such a procedure allowed us to focus parameters' estimation on the main features of the observed ERPs, while dramatically reducing noise and computational complexity.

3.6. PEB group-level connectivity analysis

In figure 8, we report the results of the greedy-search and BMA procedure on the PEB parameters associated with the average modulatory effects of the Odor (i.e. clean-air vs. isovaleric acid) and Symp (i.e. absence vs. presence of a sympathetic response) conditions on the group connectivity. These BMA parameters indicate the effect size of the average group-modulatory effect associated with the experimental variables of interest on the connectivity. Accordingly, a positive effect size of an experimental factor on a given connection indicates a strengthening of such connection, whereas a negative effect size indicates a decrease of its strength. Notably, this variation in the connectivity strength is evaluated with respect to its prior value, which is associated to the absence of a significant effect. Here, we report only those connections that show a significant modulation (i.e. $Pp > 0.95$ of having an effect size different from zero) by either Odor or Symp conditions or both. Significant connections are represented in the figure by a black bar indicating the estimated posterior effect size, and a pink error bar representing the corresponding 90% credibility interval.
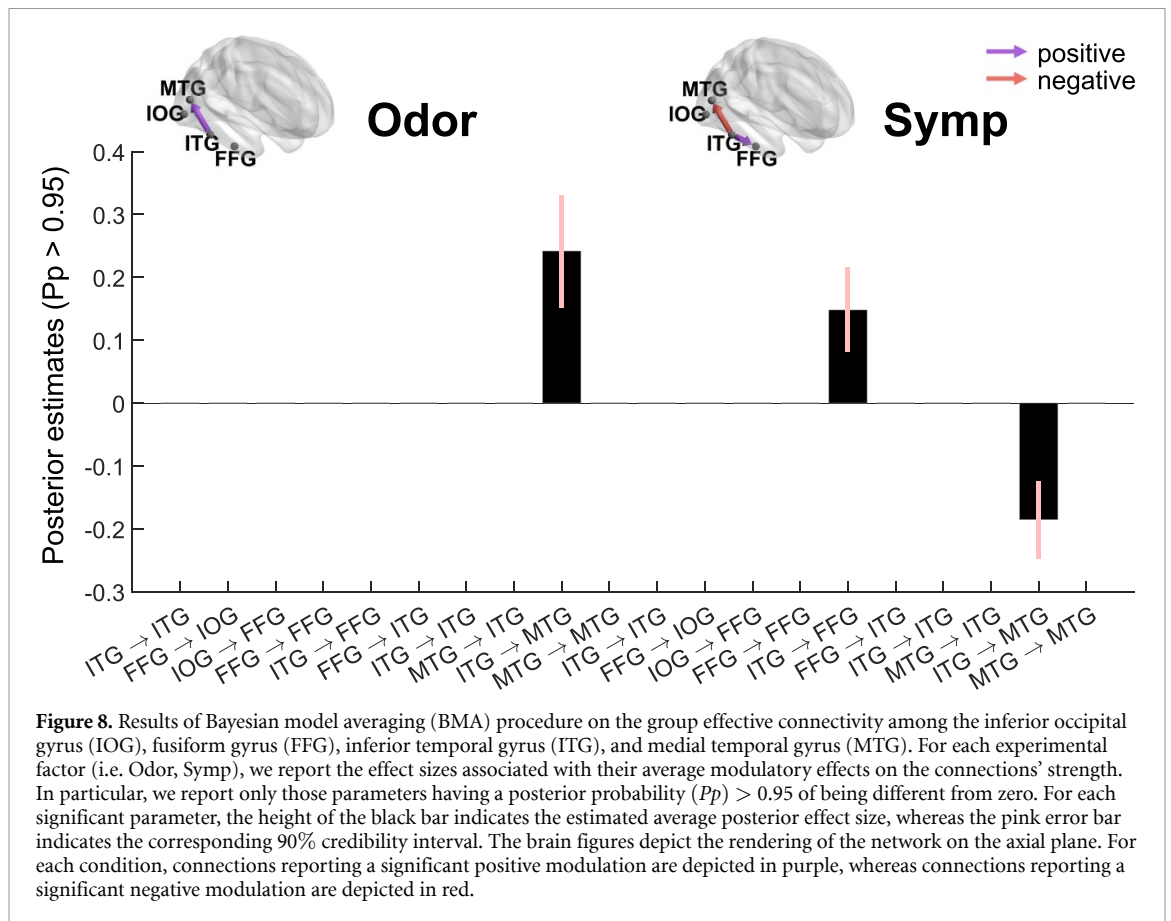
We observed a significant effect for the Odor condition on the strength of the forward connection from ITG to MTG (effect size: 0.24 ± 0.09). This indicates that the administration of isovaleric acid induced a significant (i.e. $Pp > 0.95$) excitatory effect on the strength of the ITG→MTG connection at the group level, with respect to the administration of clean-air. On the other hand, we observed a negative effect size associated with the Symp condition on the strength of the ITG→MTG connection

(effect size: -0.19 ± 0.07). This result indicates that the presence of a peripheral sympathetic response induced an inhibitory effect on the strength of the ITG→MTG connection at the group level, with respect to the absence of a sympathetic response. Finally, we also observed a positive effect size of the Symp condition on the backward connection from ITG to FFG (effect size: 0.15 ± 0.07), indicating that ITG→FFG increased in strength when peripheral sympathetic responses to faces occurred, with respect to the absence of sympathetic responses.

4. Discussion

In this study, we investigated the modulatory effect of contextual hedonic olfactory stimuli on the visual processing of neutral faces through the analysis of ERP components and effective connectivity. Particularly, we assumed that enhanced arousal to the perception of faces could play a role on their integration with olfactory stimuli, improving the SNR of the observed responses and the consequent effect size of the odors [40, 85]. To this aim, we applied a novel methodological approach exploiting EDA-driven SMNA to classify visual stimuli into two cases: i.e. 'eliciting' or 'not-eliciting' a stimulus-evoked peripheral sympathetic response. We included the outcome of this procedure as an additional experimental factor, together with the valence of contextual odors, into a standard analysis of ERP components. We further modeled observed ERPs through DCM and PEB to test for the presence of specific cortical connections being concomitantly modulated by enhanced arousal and hedonic olfactory stimuli. Our results show that the administration of unpleasant and pleasant odors (i.e. isovaleric acid and banana) was associated with a more negative N1 and VPP components' amplitude, with respect to the administration of clean air. On the other hand, although we did not find any effect of the odors on the amplitude and latency of SMNA, the occurrence of a sympathetic response time-locked to the presentations of faces was associated with a more negative N170 amplitude. On the connectivity side, we observed an increase of the connection from the ITG to MTG, during the administration of isovaleric acid. Conversely, the strength of such connection was reduced in the presence of a sympathetic response. On the other hand, sympathetic responses increased the strength of the connection from the ITG to FFG. Overall, our findings highlight the role sympathetic arousal plays on the visual processing of human faces and its multimodal integration with olfactory stimuli.

The ERP analysis revealed an effect of EDA-driven arousal on the left N170 component, irrespective of the odor condition. More specifically, the occurrence of a sympathetic response was associated with a more negative N170 component. Previous studies

Figure 8. Results of Bayesian model averaging (BMA) procedure on the group effective connectivity among the inferior occipital gyrus (IOG), fusiform gyrus (FFG), inferior temporal gyrus (ITG), and medial temporal gyrus (MTG). For each experimental factor (i.e. Odor, Symp), we report the effect sizes associated with their average modulatory effects on the connections' strength. In particular, we report only those parameters having a posterior probability (Pp) > 0.95 of being different from zero. For each significant parameter, the height of the black bar indicates the estimated average posterior effect size, whereas the pink error bar indicates the corresponding 90% credibility interval. The brain figures depict the rendering of the network on the axial plane. For each condition, connections reporting a significant positive modulation are depicted in purple, whereas connections reporting a significant negative modulation are depicted in red.

have found a significant correlation between the N170 amplitude and the perceived level of arousal associated with faces, irrespective of their valence, such that arousing stimuli were associated with increased ERP responses [34]. The N170 is considered to be the earliest marker of higher-order visual processing, marking the structural encoding of a stimulus as a face. In particular, during the N170 time window, it is hypothesized that multiple cortical processes underlie the fine-grained categorization of faces based on configural processing of their features, e.g. eyes, nose, mouth, and the spatial relationship among them [16, 86]. An alternative explanation might be that faces eliciting a sympathetic response (i.e. SMNA) could be perceived as either more threatening or more rewarding due to their intrinsic features [87, 88]. This reaction is largely subjective, as evidenced by the variation in SMNA-evoking stimuli for each participant in different odor conditions. It most probably stems from a swift bottom-up evaluation of the stimulus. The bottom–up nature of this processing is demonstrated by the fact that it occurs even during the implicit processing of stimuli, wherein the arousing features of the face do not necessarily need to be processed for the task at hand [89]. In this light, we suggest that the higher N170 amplitude observed during sympathetic responses could represent a marker of enhanced arousal elicited by salient features of faces.

In addition to the effect of arousal, we observed a more negative N1 amplitude during the administration of isovaleric acid and banana, with respect to clean air. Furthermore, we observed a more negative VPP amplitude during the administration of both isovaleric acid and banana, again with respect to clean air. These findings are in line with previous studies reporting an effect of hedonic odors on early visual ERP components [8, 11, 12]. The VPP, together with its inverse N170, is known for being particularly sensitive to faces [3, 57, 90], and it has also been implicated in contextual odor effects [11]. Hence, our findings on the VPP modulation by both the unpleasant (i.e. isovaleric acid) and pleasant (i.e. banana) odors, are in agreement with previous studies reporting an overall effect of olfactory stimuli irrespective of their valence [11]. On the other hand, a more negative N1/P1 component has been associated with the enhanced allocation of attention towards faces [3, 10]. Overall, given the ERPs results, we can state that hedonic odors generate a contextual effect and thus a top-down influence on face processing at different stages, although isovaleric acid always showed a greater effect size on the modulation of ERP responses compared to banana. In this view, we may suggest that the administration of isovaleric acid had a greater arousing effect on the early processing of visual stimuli, compared to the other odorants. This is further

corroborated by our findings on the subjective ratings of odors, showing isovaleric acid as being perceived as significantly more arousing and unpleasant compared to banana and n-butanol. Accordingly, we decided to carry out the remainder of our study focusing on the contrast between isovaleric acid and clean air.

Using DCM for ERP and PEB, we investigated the concomitant effect of Odor and Symp on the brain connectivity at the group level. The study revealed interesting results. On the one hand, we found that isovaleric acid, compared to clean air, strengthened the forward connection from the ITG to the MTG. In classical models of face processing [25, 80, 81], the MTG and the superior temporal sulcus (STS) are cortical areas specialized in processing changeable facial features (e.g. emotional expressions, gaze, lip movements). The strengthening of the connection towards these areas due to isovaleric acid may represent a crucial aspect of our study. Variable characteristics of the face are fundamental features for intra-species communication and social interaction [91]. For this reason, an interpretation of this result may consist of the fact that a negative odor can influence face processing mostly for interaction purposes. A repulsive smell would enhance the ability to interpret intentions, expressions and mental states of a possible other person (or threatening agent) in a more efficient way, bringing therefore an evolutionary advantage. On the other hand, the same connection suffered from an inhibitory effect when a simultaneous peripheral sympathetic response occurred, irrespective of the odor condition. Moreover, the occurrence of such sympathetic responses caused an excitatory effect on the backward connection from ITG to FFG. Face processing network models [80, 81] highlight the functional dissociation between the fusiform face area (in the FFG) and temporal areas. As stated above, MTG and STS are designated to process changeable facial aspects, while the FFA is crucial to process invariant aspects of the face to access information related to the identity. In particular, recent literature confirmed crucial effective connectivity among these areas, thus confirming the connections described by models of the core system of face perception [25]. Furthermore, most recent advances in the literature confirmed the specialization of the areas involved in this system [92]. According to our results, the facial information processing appears to stop at the FFG stage for faces that generate a sympathetic response, since forward connections towards the MTG are inhibited while backward connections to the FFG are enhanced. Therefore, we can speculate that the processing of faces that evoke a sympathetic response may be focused on identity-related information, to the disadvantage of emotional expressions and other changeable features. In other words, some intrinsic facial features create a sympathetic response which, in turn, may result in a top-down enhanced processing of identity. Speculatively, if a face generates a sympathetic response it is likely that this individual will feel in jeopardy, or more generally anxious. In this situation, fast processing of the face identity may represent an advantage in order to understand whether s/he is in actual danger and, in that case, adopt the appropriate fight or flight strategies connected to higher arousal. Moreover, these dynamics seem to suggest a crucial role ITG plays in processing sympathetic arousal that can be associated with odor perception. The ITG has been described as an associative area integrating information regarding face features from the FFG and IOG to process the identity of faces [93]. Furthermore, the ITG sends bidirectional projections to limbic areas involved in emotions and memory processing, such as the amygdala, hippocampus, entorhinal cortex, and to the frontal cortices [93, 94]. In this context, previous studies have reported a role for the ITG in visual short-term memory [95–97], as well as in hedonic olfactory tasks and in the perception of faces with background odor cues [75, 98]. In this light, the ITG appears to be a hub in which dissociation in different pathways for affective processing of faces are handled.

The methodology proposed in this study could represent an effective means to quantitatively study the effect of sympathetic arousal on both the ERPs and effective connectivity. Indeed, in previous studies, we adopted subjective ratings as a means to quantify arousal and investigate its central correlates at the connectivity level [71, 99]. However, affective ratings may deviate from physiological responses [71], which are supposed instead to represent an objective window on emotional stimuli processing (see e.g. [100]). Other studies instead investigated the coupling between EDA and EEG dynamics through correlation [101–104], phase and amplitude coupling [105], and coherence measures [106]. Yet, to the best of our knowledge, a methodology to investigate the effect of sympathetic arousal on the EEG effective connectivity as estimated through EDA is missing. In this light, we proposed an approach based on the identification of enhanced sympathetic arousal through the analysis of EDA and the connectivity framework of DCM for ERP. Particularly, we adopted cvxEDA as an efficient approach to recover an estimate of the hidden SMNA, and identified the time instants at which stimulus-evoked sympathetic responses have occurred. The DCM framework then allowed to investigate such effects on the effective connectivity with the highest level of physiological plausibility.

It is worth highlighting that the observed peripheral sympathetic responses could be attributed either to the effect of background olfactory stimuli, the presentation of visual faces, or the combination of both. With this regard, our EDA analysis

results did not show any significant effects of the administered background olfactory stimuli on either the amplitude, the latency, or the frequency of the sympathetic responses following the presentation of human faces. Accordingly, it is reasonable to assume that the observed peripheral sympathetic responses time-locked to the presentation of faces could be associated with the intrinsic arousing properties of the faces themselves. Thus, the proposed methodology allows accounting for two distinct, yet concomitant, effects on the EEG cortical connectivity, i.e. the modulation of contextual hedonic odors on the perception of human faces, and the modulation of enhanced sympathetic arousal elicited by the visual presentation of faces. Nevertheless, to the best of our knowledge, this is the first investigation of EDA dynamics in the scenario of the multimodal integration between visual faces and olfactory stimuli. Hence, further investigations will be necessary to corroborate this hypothesis.

The choice of focusing our DCM analysis only on the right hemisphere was supported by the literature [24, 25, 74, 78, 79, 107] and allowed us to limit the number of parameters (i.e. nodes, connections) at the advantage of less uncertainty on their estimates. However, this can be seen in contrast to the ERP analysis that revealed an effect of sympathetic arousal on the left N170 component, while no effects were observed in the right hemisphere. Nevertheless, it is worth noting that multiple sources underlie the processing of faces in the N170 (160–200) ms interval. Hence, ERP components may reflect the global activation of the face perception system, potentially leading to small or null effects [16]. In this view, DCM offers a powerful means to investigate the effect of sympathetic arousal to a deeper extent through a physiologically plausible description of how observed dynamics are associated with its underlying cortical underpinnings. Accordingly, future works should increase statistical power by including more subjects and extend our network to also include left-hemisphere ITG and MTG found during ERP inversion.

The framework proposed does not include the amplitude of the SMNA in the model. This is a limitation of the model since we cannot exclude that a potential relationship between central responses and the magnitude of the sympathetic neural bursts could exist. Yet, modeling such an effect through DCM would require to specify a single-trial within-subject modulatory input where each administered stimulus is associated to its respective level of sympathetic arousal (as quantified through the amplitude of SMNA). To the best of our knowledge, the DCM for ERP framework is limited to model between-trials effects (i.e. differences among grand-average ERPs), rather than single-trial effects. Accordingly, we limited our methodology to the evaluation of

connectivity differences in the binary case of the presence/absence of an evoked peripheral sympathetic response, without taking into account their magnitude.

SMNA responses may be triggered by a number of factors different from the perception of the designed administered stimulus (in this context, human faces). Particularly, spontaneous fluctuations, i.e. sudomotor nerve responses which stem from uncontrolled cognitive and emotional processes [39], may lead to the erroneous detection of a face-evoked peripheral sympathetic responses. While we attempted at mitigating such effects constraining stimulus-evoked SMNA bursts in the 1–5 s time window after stimulus onset [39], we cannot exclude that errors in the binary classification of the stimuli may still occur.

Another potential limitation of our methodology concerns the relationship between EDA-driven peripheral sympathetic responses and EEG central responses. Specifically, we could not explicitly include EDA dynamics into the analysis of effective connectivity, as the DCM framework only allows to model modulatory effects on the observed EEG data due to either contextual factors or properties of the administered stimuli [22]. Accordingly, nothing can be concluded about the causal relationship between EEG and EDA responses. To overcome these limitations, future studies will aim develop a framework including EDA dynamics as a representative node in the connectivity network.

5. Conclusion

In this work, we proposed a novel methodological approach based on the analysis of EDA and EEG to investigate the effect of contextual hedonic odors and sympathetic arousal on the visual processing of neutral faces. Our main findings highlighted a higher N1 component during the unpleasant odor condition, whereas enhanced arousal to faces increased the N170 component. Moreover, both factors exerted a significant modulatory effect on the effective connectivity among cortical areas involved in face processing. Particularly, the unpleasant odor strengthened the forward connection from ITG to MTG, whereas the same connection was inhibited by the simultaneous occurrence of face-evoked sympathetic responses. These results may suggest that, on the one hand, face processing in the context of an unpleasant odor are more focused on changeable facial aspects related to social interaction. On the other hand, increased arousal appears to enhance identity processing in the FFG. Future works will include SMNA dynamics as a representative node in the connectivity network, to investigate EDA-EEG causal interactions and deepen the understanding of sympathetic arousal's role on the visual-odor multimodal integration.

Data availability statement

Acknowledgments

Conflict of interest statement

The authors declare no conflict of interest.

ORCID iDs

Gianluca Rho ● https://orcid.org/0000-0002-9919-9261
Alejandro Luis Callara ● https://orcid.org/0000-0003-2767-0699
Tommaso Lomonaco ● https://orcid.org/0000-0002-1822-7399

References

[1] Syrjänen E, Fischer H, Liuzza M T, Lindholm T and Olofsson J K 2021 A review of the effects of valenced odors on face perception and evaluation *i-Perception* **12** 20416695211009552

[2] Aviezer H, Ensenberg N and Hassin R R 2017 The inherently contextualized nature of facial emotion perception *Curr. Opin. Psychol.* **17** 47–54

[3] Damon F, Mezrai N, Magnier L, Leleu A, Durand K and Schaal B 2021 Olfaction in the multisensory processing of faces: a narrative review of the influence of human body odors *Front. Psychol.* **12** 750944

[4] Li D, Jia J and Wang X 2020 Unpleasant food odors modulate the processing of facial expressions: an event-related potential study *Front. Neurosci.* **14** 686

[5] Cook S, Fallon N, Wright H, Thomas A, Giesbrecht T, Field M and Stancak A 2015 Pleasant and unpleasant odors influence hedonic evaluations of human faces: an event-related potential study *Front. Hum. Neurosci.* **9** 661

[6] Cook S, Kokmotou K, Soto V, Fallon N, Tyson-Carr J, Thomas A, Giesbrecht T, Field M and Stancak A 2017 Pleasant and unpleasant odour-face combinations influence face and odour perception: an event-related potential study *Behav. Brain Res.* **333** 304–13

[7] Cook S, Kokmotou K, Soto V, Wright H, Fallon N, Thomas A, Giesbrecht T, Field M and Stancak A 2018 Simultaneous odour-face presentation strengthens hedonic evaluations and event-related potential responses influenced by unpleasant odour *Neurosci. Lett.* **672** 22–27

[8] Syrjänen E, Wiens S, Fischer H, Zakrzewska M, Wartel A, Larsson M and Olofsson J K 2018 Background odors modulate N170 ERP component and perception of emotional facial stimuli *Front. Psychol.* **9** 1000

[9] Syrjänen E, Fischer H and Olofsson J K 2019 Background odors affect behavior in a dot-probe task with emotionally expressive faces *Physiol. Behav.* **210** 112540

[10] Adolph D, Meister L and Pause B M 2013 Context counts! Social anxiety modulates the processing of fearful faces in the context of chemosensory anxiety signals *Front. Hum. Neurosci.* **7** 283

[11] Leleu A, Godard O, Dollion N, Durand K, Schaal B and Baudouin J Y 2015 Contextual odors modulate the visual processing of emotional facial expressions: an ERP study *Neuropsychologia* **77** 366–79

[12] Steinberg C, Dobel C, Schupp H T, Kissler J, Elling L, Pantev C and Junghöfer M 2012 Rapid and highly resolving: affective evaluation of olfactorily conditioned faces *J. Cogn. Neurosci.* **24** 17–27

[13] Callara A L *et al* 2022 Human body odors of happiness and fear modulate the late positive potential component during neutral face processing: a preliminary ERP study on healthy subjects *2022 44th Annual Int. Conf. IEEE Engineering in Medicine & Biology Society* (*EMBC*) (IEEE) pp 4093–6

[14] Hartigan A and Richards A 2017 Disgust exposure and explicit emotional appraisal enhance the LPP in response to disgusted facial expressions *Soc. Neurosci.* **12** 458–67

[15] Rubin D, Botanov Y, Hajcak G and Mujica-Parodi L R 2012 Second-hand stress: inhalation of stress sweat enhances neural response to neutral faces *Soc. Cogn. Affective Neurosci.* **7** 208–12

[16] Rossion B 2014 Understanding face perception by means of human electrophysiology *Trends Cogn. Sci.* **18** 310–8

[17] Zatorre R J, Jones-Gotman M and Rouby C 2000 Neural mechanisms involved in odor pleasantness and intensity judgments *Neuroreport* **11** 2711–6

[18] Jadauji J B, Djordjevic J, Lundström J N and Pack C C 2012 Modulation of olfactory perception by visual cortex stimulation *J. Neurosci.* **32** 3095–100

[19] Friston K J 2011 Functional and effective connectivity: a review *Brain Connect.* **1** 13–36

[20] Schoffelen J M and Gross J 2009 Source connectivity analysis with MEG and EEG *Hum. Brain Mapp.* **30** 1857–65

[21] Friston K J, Harrison L and Penny W 2003 Dynamic causal modelling *Neuroimage* **19** 1273–302

[22] Kiebel S J, Garrido M I, Moran R J and Friston K J 2008 Dynamic causal modelling for EEG and MEG *Cogn. Neurodyn.* **2** 121–36

[23] Frässle S, Krach S, Paulus F M and Jansen A 2016 Handedness is related to neural mechanisms underlying hemispheric lateralization of face processing *Sci. Rep.* **6** 27153

[24] Nguyen V T, Breakspear M and Cunnington R 2014 Fusing concurrent EEG–fMRI with dynamic causal modeling: application to effective connectivity during face perception *Neuroimage* **102** 60–70

[25] Kessler R, Rusch K M, Wende K C, Schuster V and Jansen A 2021 Revisiting the effective connectivity within the distributed cortical network for face perception *NeuroImage: Rep.* **1** 100045

[26] Li J *et al* 2010 Effective connectivities of cortical regions for top-down face processing: a dynamic causal modeling study *Brain Res.* **1340** 40–51

[27] Fairhall S L and Ishai A 2007 Effective connectivity within the distributed cortical network for face perception *Cereb. Cortex* **17** 2400–6

[28] Chen C C, Henson R, Stephan K E, Kilner J M and Friston K J 2009 Forward and backward connections in the brain: a DCM study of functional asymmetries *Neuroimage* **45** 453–62

[29] Garvert M M, Friston K J, Dolan R J and Garrido M I 2014 Subcortical amygdala pathways enable rapid face processing *Neuroimage* **102** 309–16

[30] Sato W, Kochiyama T, Uono S, Matsuda K, Usui K, Usui N, Inoue Y and Toichi M 2017 Bidirectional electric communication between the inferior occipital gyrus and the amygdala during face processing *Hum. Brain Mapp.* **38** 4511–24

[31] Lang P J, Bradley M M, Fitzsimmons J R, Cuthbert B N, Scott J D, Moulder B and Nangia V 1998 Emotional arousal and activation of the visual cortex: an fMRI analysis *Psychophysiology* **35** 199–210

[32] Balconi M and Pozzoli U 2009 Arousal effect on emotional face comprehension: frequency band changes in different time intervals *Physiol. Behav.* **97** 455–62

[33] Eimer M 2000 The face-specific N170 component reflects late stages in the structural encoding of faces *Neuroreport* **11** 2319–24

[34] Almeida P R, Ferreira-Santos F, Chaves P L, Paiva T O, Barbosa F and Marques-Teixeira J 2016 Perceived arousal of facial expressions of emotion modulates the N170, regardless of emotional category: time domain and time–frequency dynamics *Int. J. Psychophysiol.* **99** 48–56

[35] Hietanen J K, Kirjavainen I and Nummenmaa L 2014 Additive effects of affective arousal and top-down attention on the event-related brain responses to human bodies *Biol. Psychol.* **103** 167–75

[36] Lang P J 1995 The emotion probe: studies of motivation and attention *Am. Psychol.* **50** 372

[37] Lang P J, Bradley M M and Cuthbert B N 1998 Emotion and attention: stop, look and listen *Cahiers Psychol. Cogn.* **17** 997–1020

[38] Balconi M and Lucchiari C 2008 Consciousness and arousal effects on emotional face processing as revealed by brain oscillations. a gamma band analysis *Int. J. Psychophysiol.* **67** 41–46

[39] Boucsein W 2012 *Electrodermal Activity* (Springer Science & Business Media)

[40] Nieuwenhuis S, De Geus E J and Aston-Jones G 2011 The anatomical and functional relationship between the P3 and autonomic components of the orienting response *Psychophysiology* **48** 162–75

[41] Frith C D and Allen H A 1983 The skin conductance orienting response as an index of attention *Biol. Psychol.* **17** 27–39

[42] Barry R J and Furedy J J 1993 Stimulus intensity and novelty interact in elicitation of the phasic electrodermal orienting response *Int. J. Psychophysiol.* **14** 249–54

[43] Spinks J A, Blowers G H and Shek D T 1985 The role of the orienting response in the anticipation of information: a skin conductance response study *Psychophysiology* **22** 385–94

[44] Greco A, Valenza G, Lanata A, Scilingo E P and Citi L 2015 cvxEDA: a convex optimization approach to electrodermal activity processing *IEEE Trans. Biomed. Eng.* **63** 797–804

[45] Zeidman P, Jafarian A, Seghier M L, Litvak V, Cagnan H, Price C J and Friston K J 2019 A guide to group effective connectivity analysis, part 2: second level analysis with PEB *Neuroimage* **200** 12–25

[46] Hummel T, Sekinger B, Wolf S R, Pauli E and Kobal G 1997 Sniffin'sticks': olfactory performance assessed by the combined testing of odor identification, odor discrimination and olfactory threshold *Chem. Sens.* **22** 39–52

[47] Naudin M, El-Hage W, Gomes M, Gaillard P, Belzung C, Atanasova B and Goel N 2012 State and trait olfactory markers of major depression *PLoS One* **7** e46938

[48] Lomonaco T, Salvo P, Ghimenti S, Biagini D, Vivaldi F, Bonini A, Fuoco R and Di Francesco F 2021 Stability of volatile organic compounds in sorbent tubes following SARS-CoV-2 inactivation procedures *J. Breath Res.* **15** 037102

[49] Ma D S, Correll J and Wittenbrink B 2015 The Chicago face database: a free stimulus set of faces and norming data *Behav. Res. Methods* **47** 1122–35

[50] Peirce J W 2007 PsychoPy-psychophysics software in Python *J. Neurosci. Methods* **162** 8–13

[51] Greco A, Valenza G and Scilingo E P 2016 Emotions and mood states: modeling, elicitation and recognition *Advances in Electrodermal Activity Processing With Applications for Mental Health* (Springer) pp 45–54

[52] Sjouwerman R and Lonsdorf T 2019 Latency of skin conductance responses across stimulus modalities *Psychophysiology* **56** e13307

[53] Delorme A and Makeig S 2004 EEGLAB: an open source toolbox for analysis of single-trial EEG dynamics including independent component analysis *J. Neurosci. Methods* **134** 9–21

[54] Mullen T R, Kothe C A E, Chi Y M, Ojeda A, Kerth T, Makeig S, Jung T-P and Cauwenberghs G 2015 Real-time neuroimaging and cognitive monitoring using wearable dry EEG *IEEE Trans. Biomed. Eng.* **62** 2553–67

[55] Makeig S, Bell A, Jung T P and Sejnowski T J 1995 Independent component analysis of electroencephalographic data *Advances in Neural Information Processing Systems* vol 8

[56] Zhang D, Liu Y, Zhou C, Chen Y, Luo Y and Urgesi C 2014 Spatial attention effects of disgusted and fearful faces *PLoS One* **9** e101608

[57] Trautmann-Lengsfeld S A, Dominguez-Borras J, Escera C, Herrmann M, Fehr T and Kiebel S 2013 The perception of dynamic and static facial expressions of happiness and disgust investigated by ERPs and fMRI constrained source analysis *PLoS One* **8** e66997

[58] Barr D J, Levy R, Scheepers C and Tily H J 2013 Random effects structure for confirmatory hypothesis testing: keep it maximal *J. Mem. Lang.* **68** 255–78

[59] Bates D, Kliegl R, Vasishth S, Baayen H 2015 Parsimonious mixed models (arXiv:150604967)

[60] Bossi F, Gallucci M, Ricciardelli P and Avenanti A 2018 How social exclusion modulates social information processing: a behavioural dissociation between facial expressions and gaze direction *PLoS One* **13** e0195100

[61] Benjamini Y and Yekutieli D 2001 The control of the false discovery rate in multiple testing under dependency *Ann. Stat.* **29** 1165–88

[62] Ashburner J *et al* 2014 *Spm12 Manual* vol 2464 (Wellcome Trust Centre for Neuroimaging) p 4

[63] David O, Kiebel S J, Harrison L M, Mattout J, Kilner J M and Friston K J 2006 Dynamic causal modeling of evoked responses in EEG and MEG *Neuroimage* **30** 1255–72

[64] Felleman D J and Van Essen D C 1991 Distributed hierarchical processing in the primate cerebral cortex *Cereb. Cortex* **1** 1–47

[65] Penny W, Iglesias-Fuster J, Quiroz Y T, Lopera F J and Bobes M A 2018 Dynamic causal modeling of preclinical autosomal-dominant Alzheimer's disease *J. Alzheimer's Dis.* **65** 697–711

[66] López J D, Litvak V, Espinosa J J, Friston K and Barnes G R 2014 Algorithmic procedures for Bayesian MEG/EEG source reconstruction in SPM *Neuroimage* **84** 476–87

[67] Litvak V and Friston K 2008 Electromagnetic source reconstruction for group studies *Neuroimage* **42** 1490–8

[68] Rolls E T, Huang C C, Lin C P, Feng J and Joliot M 2020 Automated anatomical labelling atlas 3 *Neuroimage* **206** 116189

[69] Kiebel S J, David O and Friston K J 2006 Dynamic causal modelling of evoked responses in EEG/MEG with lead field parameterization *Neuroimage* **30** 1273–84

[70] Litvak V *et al* 2011 EEG and MEG data analysis in SPM8 *Comput. Intell. Neurosci.* **2011** 1–32

[71] Rho G, Callara A L, Cecchetto C, Vanello N, Scilingo E P and Valence G A 2022 Arousal and Gender effect on olfactory cortical network connectivity: a study using dynamic causal modeling for EEG *IEEE Access* **10** 127313–27

[72] Friston K, Zeidman P and Litvak V 2015 Empirical Bayes for DCM: a group inversion scheme *Front. Syst. Neurosci.* **9** 164

[73] Friston K J, Litvak V, Oswal A, Razi A, Stephan K E, Van Wijk B C, Ziegler G and Zeidman P 2016 Bayesian model reduction and empirical Bayes for group (DCM) studies *Neuroimage* **128** 413–31

[74] Elbich D B, Molenaar P C and Scherf K S 2019 Evaluating the organizational structure and specificity of network topology within the face processing system *Hum. Brain Mapp.* **40** 2581–95

[75] Cecchetto C, Fischmeister F P S, Reichert J L, Bagga D and Schöpf V 2019 When to collect resting-state data: the influence of odor on post-task resting-state connectivity *Neuroimage* **191** 361–6

[76] Rossion B, Caldara R, Seghier M, Schuller A M, Lazeyras F and Mayer E 2003 A network of occipito-temporal face-sensitive areas besides the right middle fusiform gyrus is necessary for normal face processing *Brain* **126** 2381–95

[77] Elfgren C, van Westen D, Passant U, Larsson E M, Mannfolk P and Fransson P 2006 fMRI activity in the medial temporal lobe during famous face processing *Neuroimage* **30** 609–16

[78] Jacques C, Jonas J, Maillard L, Colnat-Coulbois S, Koessler L and Rossion B 2019 The inferior occipital gyrus is a major cortical source of the face-evoked N170: evidence from simultaneous scalp and intracerebral human recordings *Hum. Brain Mapp.* **40** 1403–18

[79] Bötzel K, Schulze S and Stodieck S R 1995 Scalp topography and analysis of intracranial sources of face-evoked potentials *Exp. Brain Res.* **104** 135–43

[80] Haxby J V, Hoffman E A and Gobbini M I 2000 The distributed human neural system for face perception *Trends Cogn. Sci.* **4** 223–33

[81] Gobbini M I and Haxby J V 2007 Neural systems for recognition of familiar faces *Neuropsychologia* **45** 32–41

[82] Rolls E T 1992 Neurophysiological mechanisms underlying face processing within and beyond the temporal cortical visual areas *Phil. Trans. R. Soc.* B **335** 11–21

[83] Uono S, Sato W, Kochiyama T, Kubota Y, Sawada R, Yoshimura S and Toichi M 2017 Time course of gamma-band oscillation associated with face processing in the inferior occipital gyrus and fusiform gyrus: a combined fMRI and MEG study *Hum. Brain Mapp.* **38** 2067–79

[84] Jamieson A J, Davey C G and Harrison B J 2021 Differential modulation of effective connectivity in the brain's extended face processing system by fearful and sad facial expressions *Eneuro* **8** ENEURO.0380-20.2021

[85] Sokolov E N 1963 *Perception and the Conditioned Reflex* (Pergamon)

[86] Maurer D, Le Grand R and Mondloch C J 2002 The many faces of configural processing *Trends Cogn. Sci.* **6** 255–60

[87] Carlson J M 2021 A systematic review of event-related potentials as outcome measures of attention bias modification *Psychophysiology* **58** e13801

[88] Calvo M G and Beltrán D 2013 Recognition advantage of happy faces: tracing the neurocognitive processes *Neuropsychologia* **51** 2051–61

[89] Monroe J F, Griffin M, Pinkham A, Loughead J, Gur R C, Roberts T P L and Christopher Edgar J 2013 The fusiform response to faces: explicit versus implicit processing of emotion *Hum. Brain Mapp.* **34** 1–11

[90] Batty M and Taylor M J 2003 Early processing of the six basic facial emotional expressions *Cogn. Brain Res.* **17** 613–20

[91] Allison T, Puce A and McCarthy G 2000 Social perception from visual cues: role of the STS region *Trends Cogn. Sci.* **4** 267–78

[92] Kosakowski H L, Kanwisher N and Saxe R 2022 Face-preferring regions in FFA, STS and MPFC have different functions *Proc. Annual Meeting of the Cognitive Science Society* vol 44

[93] Tovée M J and Cohen-Tovée E M 1993 The neural substrates of face processing models: a review *Cogn. Neuropsychol.* **10** 505–28

[94] Van Hoesen G W 1982 The parahippocampal gyrus: new observations regarding its cortical connections in the monkey *Trends Neurosci.* **5** 345–50

[95] Fuster J M 1990 Inferotemporal units in selective visual attention and short-term memory *J. Neurophysiol.* **64** 681–97

[96] Iwai E, Osawa Y and Okuda H 1990 Monkey inferotemporal cortex as a long-term visual memory area *Vision, Memory and the Temporal Lobe* (Elsevier) pp 1–12

[97] Miyashita I 1990 Associative representation of visual long-term memory in the neurons of the primate temporal cortex *Vision, Memory and the Temporal Lobe* (Elsevier) pp 75–88

[98] Riley J D, Fling B W, Cramer S C and Lin J J 2015 Altered organization of face-processing networks in temporal lobe epilepsy *Epilepsia* **56** 762–71

[99] Rho G, Callara A L, Vanello N, Gentili C, Greco A and Scilingo E P 2021 Odor valence modulates cortico-cortical interactions: a preliminary study using DCM for EEG *2021 43rd Annual Int. Conf. IEEE Engineering in Medicine & Biology Society* (*EMBC*) (IEEE) pp 604–7

[100] LeDoux J 1998 *The Emotional Brain: The Mysterious Underpinnings of Emotional Life* (Simon and Schuster)

[101] Mobascher A, Brinkmeyer J, Warbrick T, Musso F, Wittsack H J, Stoermer R, Saleh A, Schnitzler A and Winterer G 2009 Fluctuations in electrodermal activity reveal variations in single trial brain responses to painful laser stimuli-A fMRI/EEG study *Neuroimage* **44** 1081–92

[102] Stuldreher I V, Thammasan N, Van Erp J B and Brouwer A M 2020 Physiological synchrony in EEG, electrodermal activity and heart rate detects attentionally relevant events in time *Front. Neurosci.* **14** 575521

[103] Posada-Quintero H F and Chon K H 2019 Phasic component of electrodermal activity is more correlated to brain activity than tonic component *2019 IEEE EMBS Int. Conf. on Biomedical & Health Informatics* (*BHI*) (IEEE) pp 1–4

[104] Lim C, Barry R, Gordon E, Sawant A, Rennie C and Yiannikas C 1996 The relationship between quantified EEG and skin conductance level *Int. J. Psychophysiol.* **21** 151–62

[105] Kroupi E, Vesin J M and Ebrahimi T 2013 Phase-amplitude coupling between EEG and EDA while experiencing multimedia content *2013 Humaine Association Conf. on Affective Computing and Intelligent Interaction* (IEEE) pp 865–70

[106] Ural G, Kaçar F and Canan S 2019 Wavelet phase coherence estimation of EEG signals for neuromarketing studies *NeuroQuantology* **17** 112–20

[107] Walla P 2008 Olfaction and its dynamic influence on word and face processing: cross-modal integration *Prog. Neurobiol.* **84** 192–209